Journal of Oil, Gas and Petrochemical Technology 10(2): 137-152, Winter and Spring 2023

RESEARCH PAPER

Predicting Production of Shale Gas Reservoirs: Impact of Hydraulic Fracture Geometry

***Alireza Sadeghinia*[1], *Mohammad Torkaman*[2,*]**

[1] *Department of Chemical Engineering, School of Chemical and Petroleum Engineering, Shiraz University, Shiraz, Iran*

[2] *Department of Chemical Engineering, Faculty of Engineering, Shahid Chamran University of Ahvaz, Ahvaz, Iran*

ARTICLE INFO

Article History:
Received 08 June 2023
Revised 25 November 2023
Accepted 04 December 2023

Keywords:
Computational fluid dynamics (CFD)
Discrete fracture model (DFM)
Fractured horizontal well
Hydraulic fracture
Numerical simulation

ABSTRACT

The present research used a numerical simulation technique known as the Discrete Fracture Model (DFM) to examine the propagation of shale gas in fractured porous media. It employed a novel mathematical model for seepage flow, incorporating the application of the 'cubic law' for flow in fractures and Darcy's law for the seepage flow in the matrix. The impact of fracture aperture on flow behavior was simulated by solving a set of nonlinear, partial, differential equations using the finite element method (FEM). Through this work, a sensitivity analysis of the significant parameters, including hydraulic fracture numbers and permeability, hydraulic fracture aperture, and wellbore length, on the productivity of a shale gas reservoir was conducted. Hydraulic fracture permeability with increasing oil production (more than twice) had the greatest effect on the wellbore productivity. Furthermore, the simulation results showed that augmenting the number of hydraulic fractures from 4 to 15 resulted in a production increase of over twofold. Also, it was observed that the production rate increased due to the existence of a positive correlation between the fracture aperture size and the drainage area. The outcome of this research showed the significance of hydraulic fracture characteristics and its ensuing effects on the productivity and feasibility. In order to validate the accuracy of the numerical model, the pressure distribution in a single fractured reservoir was compared with the pressure contour of a phase field discrete fracture model (PFDFM). The results indicated that the proposed method (FPM) was precise, convergent, and extremely promising.

How to cite this article
Sadeghinia A, Torkaman M., Predicting Production of Shale Gas Reservoirs: Impact of Hydraulic Fracture Geometry, Journal of Oil, Gas and Petrochemical Technology, 2023; 10(2): 137-152. DOI:10.22034/JOGPT.2024.401315.1121.

1. INTRODUCTION

Current research focuses on the fractured reservoirs because the majority of oil in the Middle East, including Iran, is found in the fractured reservoirs [1]. Examination of fluid flow in heterogeneous porous media, which usually includes many natural or artificial fractures, is full of challenges. This is because the production rate in naturally fractured reservoirs is highly affected by the aperture of fractures, orientation, permeability, and porosity [2], [3]. Consequently, wellbore productivity calculations and forecasts need precise knowledge of the reservoir conditions.

* *Corresponding Author Email: M.torkaman@scu.ac.ir*

Given the substantial impact of fracture on flow behavior, modeling fluid flow in fractured porous media has received considerable attention in recent years [4], [5]. According to the studies, several methods have been proposed by researchers to describe the flow behavior in fractured reservoirs, including embedded discrete fracture model (EDFM) [6], [7], extended finite element method (XFEM) [8-10], finite element method (FEM) [11-13], finite volume method (FVM) [14-16] and displacement discontinuity method (DDM) [17], [18]. Among these models, the FEM is the most effective computer-based method ever devised to address engineering problems. It has a significant advantage in reservoir simulation in that a complex geometric domain can be discretized with a maximum number of mesh points [19]. For instance, Mi et al., [20] employed FEM to study the influence of both natural and hydraulic fracture aperture on the oil production rate. They observed that a wider fracture aperture resulted in more oil production. The findings of Zhang et al., [21] showed that the productivity of horizontal wells was significantly influenced by the angle between the fracture and the wellbore. Furthermore, there was an observed correlation between the rise in fracture aperture and the subsequent increase in the production rate. The impact of hydraulic fracture numbers on well production rate was found to be insignificant, likely attributed to the presence of interfaces between the fractures. Ozkan et al., [22] examined the performance of fractured horizontal wells in conventional and unconventional reservoirs using the trilinear flow model. Their findings demonstrated that a reduction in hydraulic fracture spacing decreased the productivity of the well. Besides, the role of permeability in productivity in the fracture network was less significant than the density of the fracture network. The discerite fracture model consists of several fracture networks; hence, providing a more accurate representation of the reservoir. Using this model to simulate the process of shale gas development is more accurate to the actual situation [23]. Zhao et al., [24] developed an embedded discrete fracture model (EDFM) for a multi-stage fractured horizontal well. Based on their results, an increase in the length of horizontal wells, the number of hydraulic fractures, and the number of natural fractures connected to hydraulic fractures increase the oil production rate. An innovative fracturing reservoir simulator was developed by Cao et al., [25], [26] to evaluate the effect of fracture networks on well productivity. Based on their observations, optimal cluster spacing can maximize the contact area between the fractures and reservoirs while maintaining the highest production rate. Also, in another research they showed that the simulation results that were consistent with the properties of the natural fracture network were determined by the study of post-frac core samples. Ranjbar et al., [27-29] examined the impacts of faults and fractures on the pore pressure during fluid flow through a deformable porous medium isothermally and non-isothermally by using a coupled fluid flow-geomechanical model. Iranmanesh and Pak [30] proposed EFG (element free Galerkin) method for the thermo-hydromechanical modeling of a saturated porous medium. In addition, they reported some guidelines to select the scale and penalty factors for solving thermo-hydro-mechanical THM problems. To the best of our knowledge, there have been few studies which thoroughly examine the combined impact of hydraulic fracturing and discrete natural fracture networks on the extraction of shale gas. Ahmadi et al., [31-36] investigated the performance of the ZnO−γAl2O3 injection with smart water to improve the oil recovery. Based on their results, the concentration of SMW+300 ppm ZnO−γAl2O3 nanoparticles reached 31 from 161°. This research aimed at scrutinizing the pressure variation of shell gas more clearly. Therefore, two-dimensional cut lines were considered and pressure fluctuation in the natural fractures, horizontal well and hydraulic fractures were evaluated. Besides, to examine the flow behavior in a random naturally fractured reservoir, the impacts of hydraulic fracture number and permeability on the hydrocarbon production were addressed. Finally, in order to validate the DFM, a simulation of fluid flow in a single vertical FPM was conducted, and the results were compared to the phase field discrete

fracture model (PFDFM).

2. Numerical Model Consideration

2.1. Model Description

Figure 1 depicts a schematic of a discrete fracture network. The geometry in Figure 2 (I) corresponding to a two-dimensional rectangular domain, with dimensions of 250 × 150 m^2, was created with COMSOL Multiphysics 5.5. The geometrical model was discretized by random triangles and unstructured elements, as illustrated in the figure. As can be seen in Figure 2 (II), around the interconnection of hydraulic and natural fractures, a very high mesh density (shown in blue) is required to track flow behavior accurately. It contains 52 fractures, which consist of 48 natural fractures and 4 hydraulic fractures.

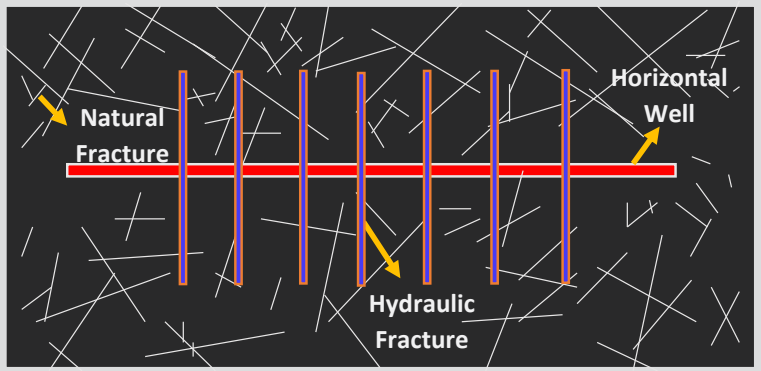

Figure 1. Geometrical demonstration of a discrete fracture network

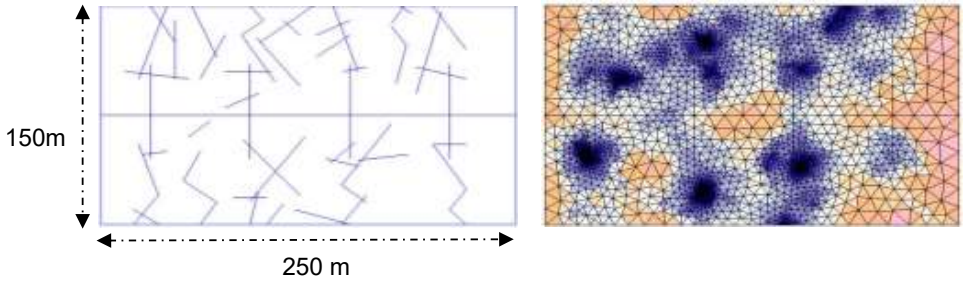

Figure 2. (I). The schematic of geometry (II). The geometrical discretization of the model

Table 1. The parameter of the CFD model [21]

Parameter	Value	Unit
Matrix porosity	0.3	[Dimensionless]
Matrix permeability	1	[mD]
Fluid compressibility	4.4×10^{-10}	[1/Pa]
Matrix compressibility	1×10^{-8}	[1/Pa]
Storage coefficient of the fracture	4.4×10^{-10}	[1/Pa]
Aperture of the natural fracture	1×10^{-5}	[m]
Aperture of the hydraulic fracture	1×10^{-3}	[m]
Viscosity	0.6	[cP]
Inlet pressure	5×10^{5}	[Pa]
Outlet pressure	3×10^{5}	[Pa]

Only production from the reservoir flows through the hydraulic fractures that connect to the horizontal well is represented by the blue line in the center of the model. It should be noted that hydraulic fractures have a larger aperture, making them more permeable than the natural fractures. The flow direction is from the perimeter to the center. The wellbore stands as the outlet, and other boundaries such as top and bottom edges are considered as the inlet edges. The information of matrix and fluid properties used for simulation is given in Table 1 [21].

2.2. DFM Assumptions

During the development of the model, numerous assumptions were made in accordance with the properties and features of shale gas formations and the flow behavior:

- Flow of fluid in the wellbore takes place through fractures that connect to the well, whereas the contribution of the matrix is disregarded.
- The drainage area of the horizontal well has a rectangular shape.
- The fluid is compressible.
- Isothermal and single-phase flow.

2.3. The Mathematical Model

Modeling of gas flow in FPM necessitates the solution of the system of equations for matrix and fracture. In this model, fluid flows through the matrix follows Darcy's law whereas flow in the fracture follows fracture flow, which is known as the Cubic Law. Time-dependent flow in the matrix, which is described by Darcy's law, is written as [20], [37]:

$$\rho S \frac{\partial P}{\partial t} + \nabla \cdot (\rho u_m) = 0 \quad (1)$$

where ρ represents the fluid density, (SI unit: kg/m^3); S represents the matrix storage coefficient, (SI unit: 1/Pa); P denotes the pressure, (SI unit: Pa); μ denotes the fluid viscosity, (SI unit: cp); u_m denotes Darcy velocity (SI unit: m/s). As porous medium and fluids are compressible, the matrix storage coefficient S is given by:

$$S = C_g \varphi + C_m(1-\varphi) \quad (2)$$

where φ is the matrix porosity (dimensionless), Yang Shenglai and Junzhi's formula for gas isothermal compressibility (SI unit: 1/Pa) is as follows [38]:

$$C_g = -\frac{1}{V}\left(\frac{\partial V}{\partial P}\right) \quad (3)$$

where v is the volume of gas (SI unit: m^3). The pressure sensitivity has been ignored, and due to the constant production pressure, the seepage flow occurs in a steady condition. The fluid flow in porous media obeys Darcy's Law, in which the fluid velocity (u_m) can be expressed as follows [20]:

$$u_m = -\frac{K_{app}}{\mu_g}\nabla P \quad (4)$$

$$K_{app} = C_g D \mu_g + F K_\infty \quad (5)$$

where k_{app} (SI unit: mD) represents the apparent matrix block permeability that couples gas diffusion and gas slippage, C_g is gas compressibility (SI unit: 1/Pa), D is diffusion coefficient (SI unit: m^2.s^{-1}), and F represents gas slippage correction coefficient. Based on the mathematical model represented above, fractures consist of a series of interior boundaries through which oil flows. Typically, flow across or normal to a boundary is defined as opposed to along it. Hence, fracture flow boundary conditions are employed to define flow along the fractures and boundaries. According to the flow boundary conditions, the velocity equation in fracture conforms to a modification of the matrix block law known as the Cubic law. Thus, the equation coefficients are changed in a way that, due to the relatively small thickness of the fracture, there is the least resistance to the flow in the fracture. The modeling of fluid flow in the fractures is analogous to the modeling of flow in a porous medium based on Equation (1). To ensure dimensional compatibility between the fracture and matrix, the fracture aperture is added to the equation. Therefore, the governing equation in the fracture can be expressed as follows [21]:

$$\rho S_f w_f \frac{\partial P}{\partial t} + \nabla \cdot (\rho u_f) = 0 \quad (6)$$

where S_f is the fracture storage coefficient,

(SI unit: 1/Pa); is the fracture aperture, (SI unit: m). Due to the fact that fracture aperture appears in the fracture flow equation, the variable represents the volume flow rate per unit fracture length in the fracture [SI unit: m^2/s], which is defined as follows [20]:

$$u_f = -\frac{K_f}{\mu_g} w_f \nabla P \tag{7}$$

$$\rho = \frac{M}{RT}\frac{P}{Z} \tag{8}$$

The reservoir temperature is denoted by T (293.15, SI unit: K), the average molecular weight of the gas is represented by M (SI unit: kg/mol), and the universal gas constant is symbolized by R (8.314, SI unit: J/mol · K). The estimation of the Z-factor (Dimensionless) can be achieved by the utilization of the Equation of State (EOS) or by employing correlations specifically designed for gas mixtures. The Z-factor is determined in this research by employing an explicit correlation proposed by Mahmoud et al., [39], which relies on the pseudo-reduced pressure (P_{pr}) and pseudo-reduced temperature (T_{pr}) [40].

$$\begin{aligned} Z = {} & (0.702e^{-2.5Tpr})(p_{pr}{}^2) - \\ & (5.524e^{-2.5Tpr})(P_{pr}) + \\ & (0.044T_{pr}{}^2 - 0.164T_{pr} + 1.15) \end{aligned} \tag{9}$$

One benefit of employing explicit correlation is the avoidance of solving higher order equations with regard to the Z-factor. This is advantageous as such equations typically yield many solutions and require increased computational resources.

The parameter of is related to the fracture aperture by Cubic Law as [20]:

$$K_f = \frac{{w_f}^2}{12} \tag{10}$$

2.4. Boundary Conditions

The boundary condition equations should be given in order to make the problem solvable. According to the model, the wellbore serves as the outflow. The top and bottom reservoir boundaries are regarded as inlet edges, whereas the other reservoir boundaries are considered as other edges. There is no flow through the other edges.

$P = P_0$ Inlet edge (11)

$P = P_{outlet}$ Outlet edge (12)

$n.u = 0$ Other edges (13)

2.5. Initial Conditions

The pressure denoted as P_0 in Equation (14) represents the initial pressure throughout the whole model, with the exception of the outlet edge where it represents the pressure at the bottom hole during the entire simulation phase.

$P_{initial} = P_0$ Whole model (14)

3. Results and Discussion

On the basis of DFM, the effects of the hydraulic fracture aperture, permeability, and numbers on the performance of the wellbore productivity were analyzed. Furthermore, the influence of wellbore length on the oil production rate was addressed in this work. In this section, the pressure and velocity distribution in a horizontally fractured well is examined, and then a sensitivity analysis is performed. Figure 3 illustrates how the pressure and velocity gradients vary as a result of fluid flow from the inlet to the wellbore. The fluid flow into the horizontal well can be categorized into two primary pathways: firstly, from natural fractures to hydraulic fractures and subsequently into the horizontal well; and secondly, from either natural fractures or hydraulic fractures directly into the horizontal well. This implies that fractures serve as the crucial conduits for fluid flow, and the characteristics of these fractures significantly influence the extraction of shale gas.

Fluid flow in FPM follows two distinct paths: from natural fractures or hydraulic fractures into the horizontal well; and from natural fractures to hydraulic fractures and then into the horizontal well, indicating that fractures play an important role in the fluid flow. To observe the pressure fluctuation in natural fracture, hydraulic fracture, and in the horizontal well more intuitively, the two-dimensional cut lines EF and GH are considered in the model (as

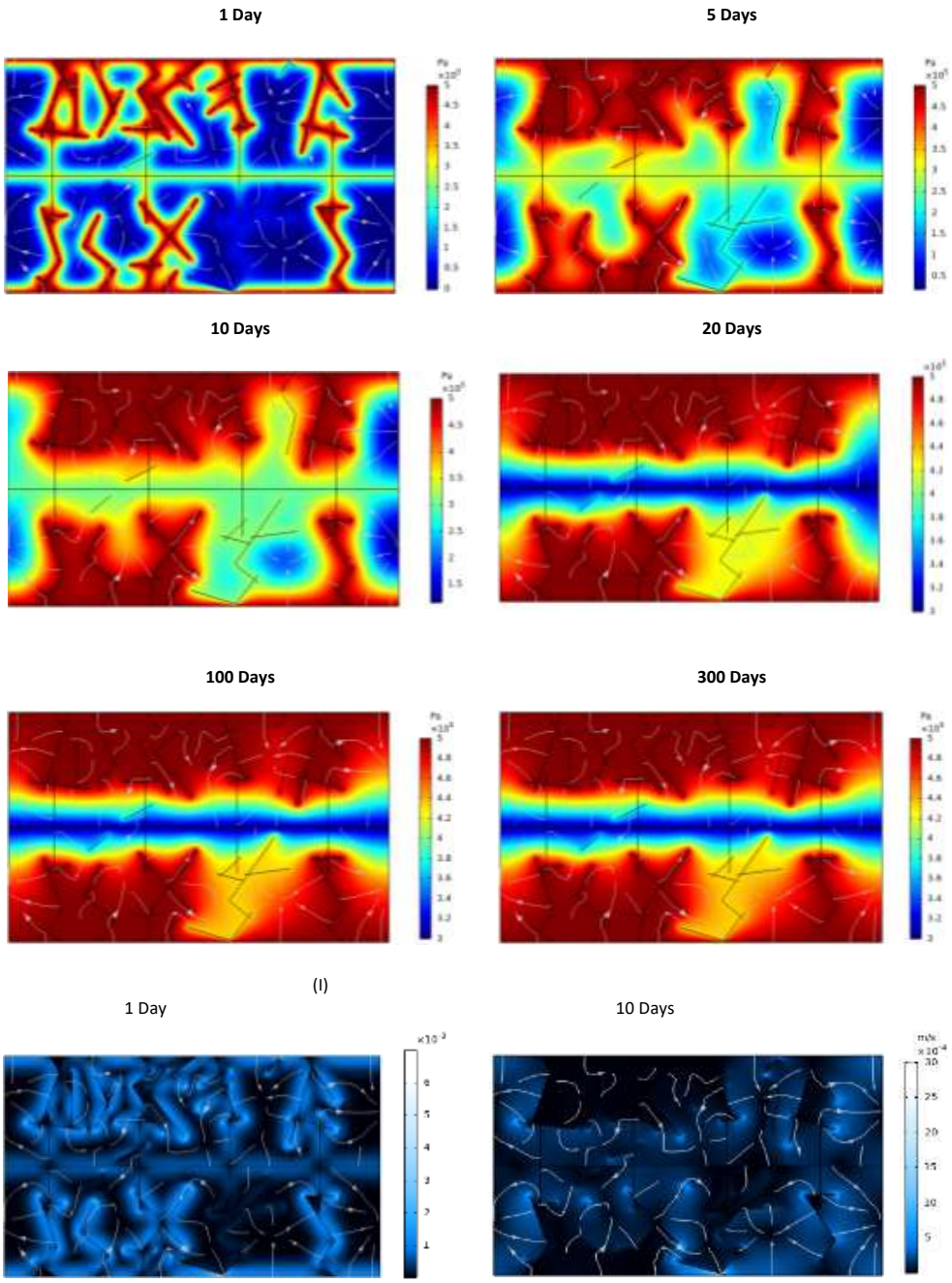

Figure 3. (I). Pressure distribution (II). Velocity distribution

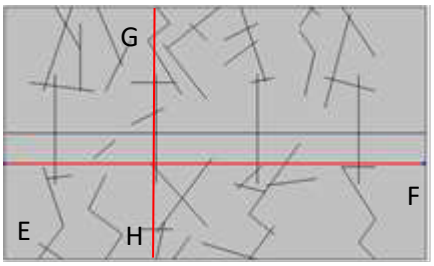

Figure 4. Schematic diagram with two-dimensional cut lines

represented in Figure 4).

As can be seen in Figure 5, the hydraulic fracture has a lower pressure than the matrix. Due to greater porosity and permeability, the resistance in hydraulic fractures is considerably lower than in the matrix. The trend in Figure 5 is consistent with the previous findings of Liu et al. [41]. The pressure variation in Figure 6 shows that pressure fluctuation mainly occurs in the EF cut line. From the figure, four peaks represent pressure in each hydraulic fracture, and it can be inferred that the higher permeability of the hydraulic fracture causes the pressure fluctuation in the hydraulic fracture to be always higher than in a natural fracture. Furthermore, the narrower the hydraulic fracture aperture, the faster the pressure drop occurs.

As Figure 7 shows, the production rate dramatically decreases after 50 days and reaches a constant value after 250 days. With the start of production, the reservoir pressure has declined, which has resulted in a decrease in the wellbore production.

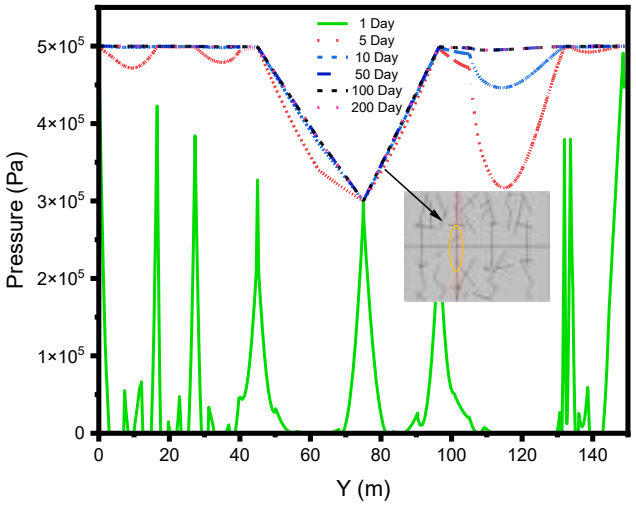

Figure 5. Pressure fluctuation at GH cut line

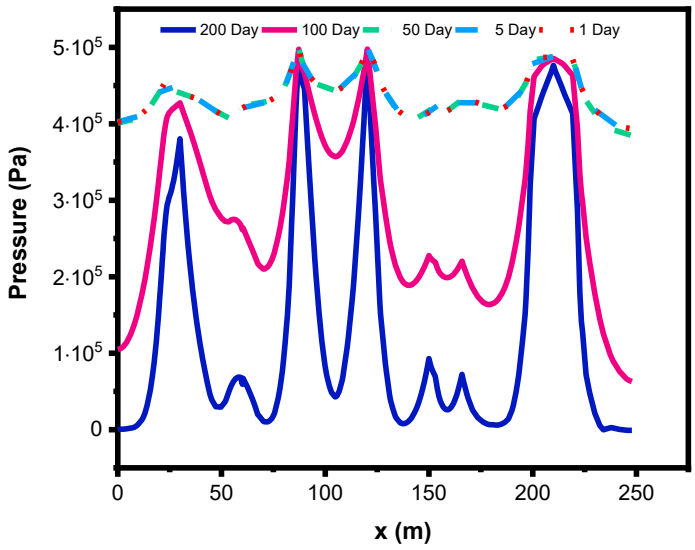

Figure 6. Pressure fluctuation at EF cut line

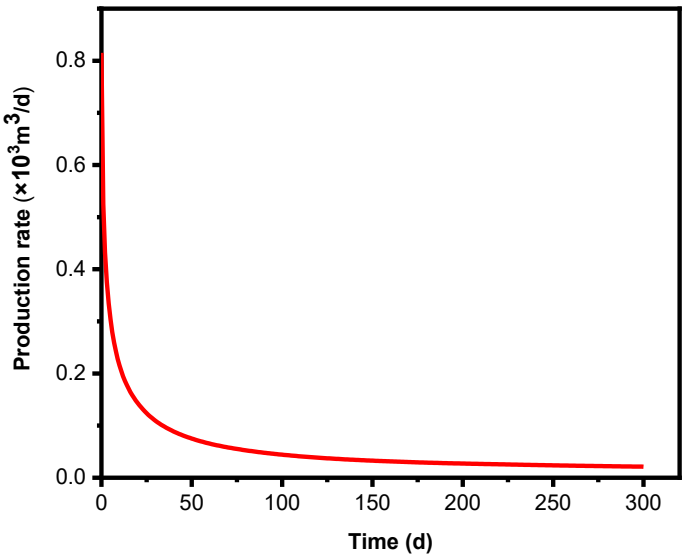

Figure 7. Production rate versus time

3.1. Impact of Aperture of Natural Fractures on Pressure Distribution

Comparing pressure profiles in cases 1 and 2 (The information of each case tabulated in Table 2) as demonstrated in Figure 8, natural fractures aperture impacts are significant when the hydraulic fracture aperture remains $1x10^{-5}$ m. The results indicate that the larger the fracture aperture, the larger the drainage area, particularly for natural fractures, which make up a significant portion of the fracture system. Therefore, if we want to increase production, we will need higher conductivity and wider fractures, and we can improve fracture flow capacity by increasing fracture aperture when horizontally fracturing the reservoir. The results are quite in agreement with the findings reported by Mi et al. [20].

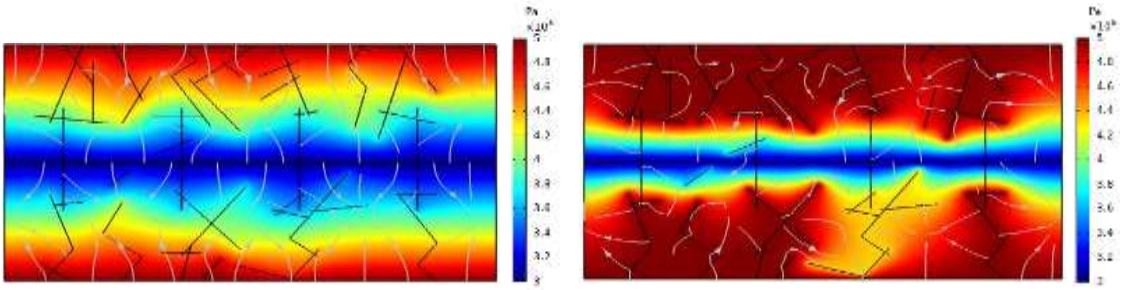

Figure 8. Pressure variation under different hydraulic fracture apertures

Table 2. Natural and Hydraulic fractures aperture in different cases

Case number	Case 1	Case 2
Hydraulic fracture aperture (m)	1×10^{-5}	1×10^{-5}
Natural fracture aperture (m)	1×10^{-4}	1×10^{-3}

3.2. Fracture Aperture

The impact of fracture aperture on shale gas production was examined. The production rate increased with an increment fracture aperture, as shown in Figure 9. When the fracture aperture rised from 0.00001 to 0.000034 m, the increment of oil production was greater than twice. According to the Cubic Law formula, an increase in the fracture aperture causes higher permeability and, consequently, an increased production rate. The results are consistent with the findings of Zhang et al. [21] and Liu et al. [41].

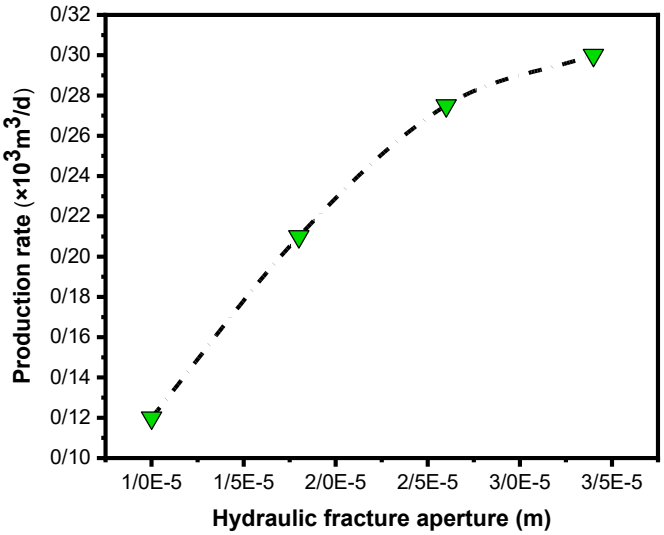

Figure 9. Production rate under various hydraulic fracture apertures

3.3. Number of Hydraulic Fractures

In this section, the effect of hydraulic fractures on well productivity is investigated. The increase in the number of hydraulic fractures leads to changes in pressure distribution, as noted by Liu et al., [41]. Consequently, there is a corresponding rise in the production rate with an increasing number of fractures. The hydraulic fracturing process generates additional flow channels, resulting in an augmented fluid flow through the fractures and into the wellbore as the number of fractures escalates. It should be noted that the production rate eventually reaches almost a constant value due to the limited capacity of fluid streaming from the matrix to the fracture. Actually, when the hydraulic fracture numbers increase continually, interferences between fractures will be generated, thus the production rate will be of a specific value. According to Figure 10, the production rate is 0.12, 0.34, 0.342, and 0.354 m^3 when the number of fractures is 4, 8, 12, and 15, respectively. According to the figure, the results agree well with those obtained by Liu et al., [41] and Zhang et al., [10].

3.4. Hydraulic Fracture Permeability

Hydraulic fractures play a crucial role in establishing a connection between the wellbore and the formation; consequently, the economic output of each well is highly dependent on the conductivity of these fractures. Therefore, a higher fracture permeability results in a higher flow rate, which causes more oil to travel into the wellbore. Figure 11 demonstrates that the production rate becomes more than double when the permeability of a hydraulic fracture is increased from 8.3 x 10^{-9} to 8.3 x 10^{-8} m^2.

3.5. Wellbore Length

The influence of the length of the horizontal well is addressed in this study, and the results show that (Figure 12) by increasing the wellbore length from 180 to 250 m, the

production rate rises by 14.7%. It can be concluded that the hydrocarbon production increases with the length of the horizontal well and, consequently, with the length of the long axis of the ellipse quasi-radial flow. The results are in good agreement with those reported by Wang et al., [40].

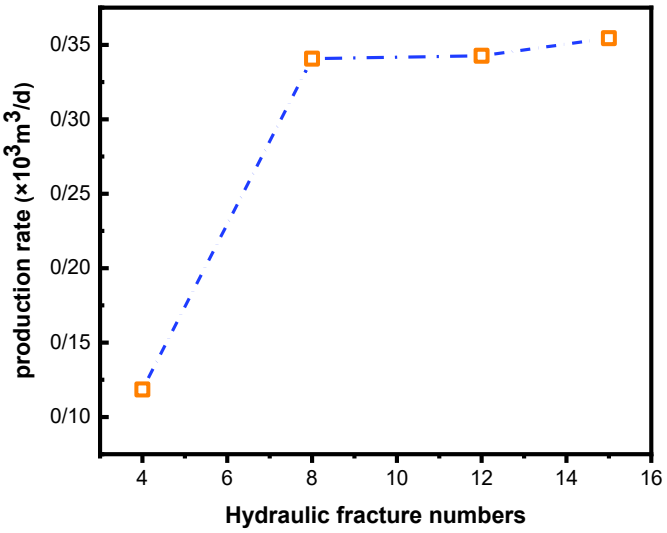

Figure 10. The effect of hydraulic fracture numbers on production rate

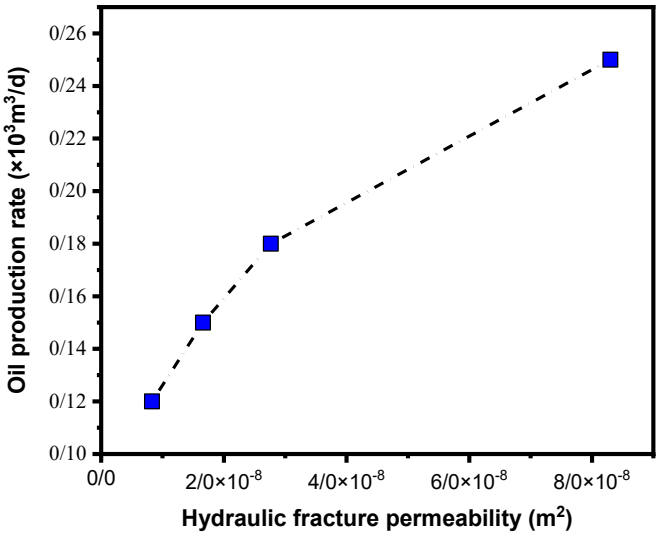

Figure 11. The effect of hydraulic fracture permeability on oil production rate

3.6. Validation of DFM

The performance of proposed model for simulating fluid flow in a naturally fractured reservoir was assessed with PFDFM developed by Zeng et al., [42]. For this purpose, a vertical fracture reservoir was considered. The former case is demonstrated in Figure 13.

The geometry corresponding to vertical fracture has a length of 0.6 m and a width of 0.5 mm. In addition, the pressure in the inlet and outlet boundaries are fixed at 1 and 2 MPa respectively. Other parameters consist of fluid

viscosity μ = 103 Pa.s, length parameter L = 1 m, and matrix permeability $K_m = 10^{-12}$ m^2. These parameters remained unchanged for the following scenario. The pressure distribution in a single vertical fracture modeled by DFM and PFDFM is depicted in Figure 14. From the figure, the pressure contour of DFM is consistent with PFDFM.

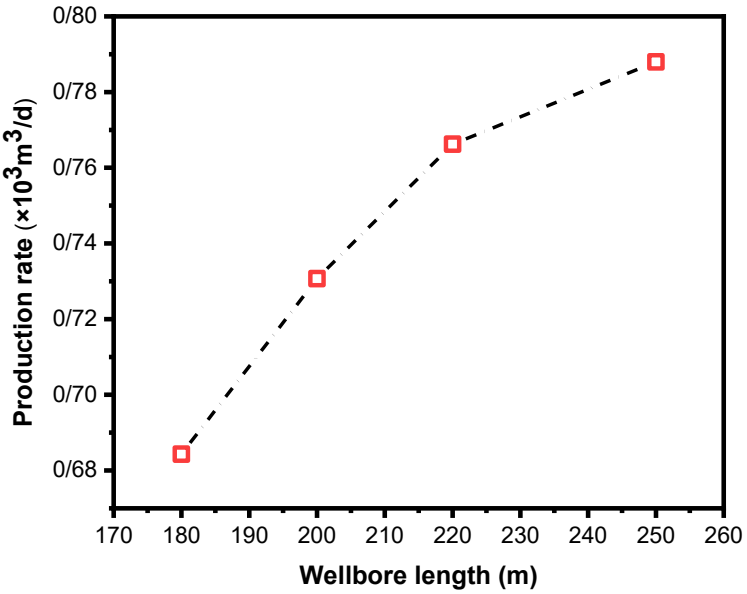

Figure 12. Production rate versus wellbore length

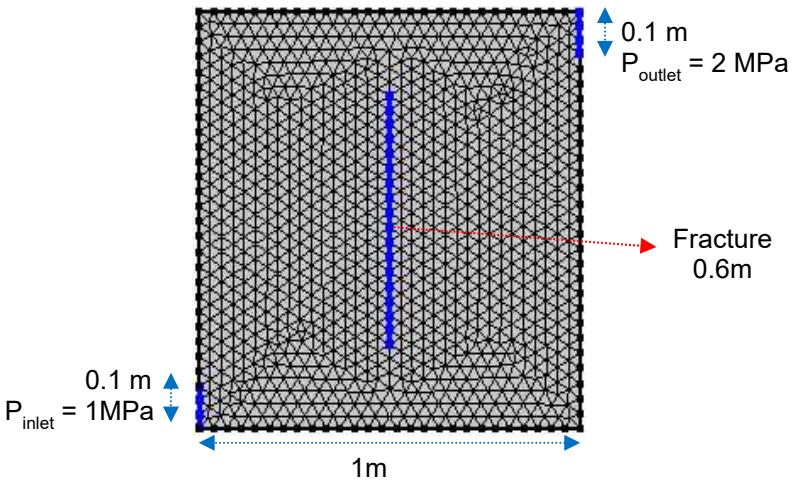

Figure 13. Schematic of the model with vertical fracture

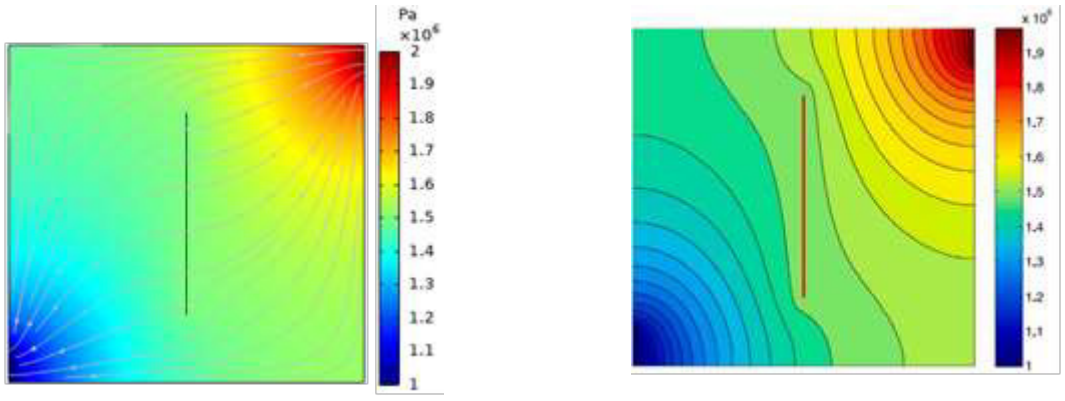

(I) **(II)**

Figure 14. Comparison pressure contours. (I) DFM result, (II) PFDFM result presented by Zeng et al., [42]

4. Conclusions

The simulation approach was carried out by employing a mathematical model in which fluid flow in the matrix follows Darcy's Law while meeting Cubic Law in fracture. A sensitivity analysis indicated that the number of hydraulic fractures and the permeability of the wellbore played a significant role in the production rate. As the permeability was proportional to the aperture of the fissure, an increase in the aperture resulted in a production increase that was more than twice. From the perspective of the production rate variation, increasing the number of hydraulic fractures from 4 to 15 led to a rise in wellbore productivity of 198%. However, by increasing the number of hydraulic fractures continuously, the production rate tended to be unchanged, which might be because of the interference of the fractures created. Moreover, the evaluation of the impact of wellbore length on the production rate shows that increasing the wellbore length by 38% resulted in rising wellbore productivity by 14.7%. The performance of the DFM was validated against the PFDFM by calculating the pressure distribution in a single vertical fracture reservoir. The results depicted that DFM can accurately model the fluid flow in fractured reservoirs.

Nomenclature	
S	Storage coefficient [1/Pa]
P	Pressure [Pa]
t	Time [s]
u_f	Volume flow rate in fracture [m^2/s]
u_m	Volume flow rate in matrix [m/s]
C_g	Gas compressibility [1/Pa]
C_m	Matrix compressibility [1/Pa]
V	Volume [m^3]
K_f	Fracture permeability [mD]
K_∞	Absolute permeability [mD]
Kapp	Apparent permeability [mD]
D	Gas diffusion coefficient [$m^2.s^{-1}$]
F	Gas slippage correction coefficient
w	Fracture aperture [m]
M	Gas molar mass [Kg/mol]
Z	Compression factor
T	Shale gas reservoir temperature [K]
R	Universal gas constant, 8.314 [J/mol.K]
P_{pr}	pseudo-reduced pressure
T_{pr}	pseudo-reduced temperature
Greek letters	
ρ	Density [Kg/m^3]
μ	Viscosity [Pa.s]
ϕ	Prosity [Dimensionless]
Abbreviations	
CFD	Computational fluid dynamics
DFM	Discrete fracture model

Abbreviations	
FPM	Fracture porous media
PFDFM	Phase-field discrete fracture model
EFG	Element free Galerkin
EDFM	Embedded discrete fracture model
FVM	Finite volume method
DDM	Displacement discontinuity method
FEM	Finite element method
XFEM	Extended finite element method

References

1. Taheri Shakib, J. and Jalalifar, H., 2012. Effect of hydraulic fracture on the fractured reservoir based on the connection with natural fractures. Journal of Chemical and Petroleum Engineering, 46(2): 123-133.
2. Khanal, A., Weijermars, R., 2020. Comparison of flow solutions for naturally fractured reservoirs using Complex Analysis Methods (CAM) and Embedded Discrete Fracture Models (EDFM): Fundamental design differences and improved scaling method. Geofluids 2020, 1-20.
3. Arias Ortiz, D.A., Klimkowski, L., Finkbeiner, T. and Patzek, T.W., 2021. The effect of hydraulic fracture geometry on well productivity in shale oil plays with high pore pressure. Energies, 14(22), p.7727.
4. Liu, J., Zhou, Y. and Chen, J., 2021. A Two-Dimensional Partitioning of Fracture–Matrix Flow in Fractured Reservoir Rock Using a Dual-Porosity Percolation Model. Energies, 14(8): 2209.
5. Dawei, Z., Yongle, H., Mingyue, C., Yandong, C., LIANG, C., Wenxin, C., Yanhui, H., Xiaoyong, W., Hui, C., Xiang, L., 2020. Productivity simulation of hydraulically fractured wells based on hybrid local grid refinement and embedded discrete fracture model. Petroleum Exploration and Development 47, 365-373.
6. Xie, H., Torres, M.F., Cheng, P., Yu, W., Xin, Y., Miao, J. and Cheng, M., 2022. A new-generation Embedded Discrete Fracture Model calibration workflow applied to the characterization of complex naturally fracture reservoir. Petroleum Research, 7(1), pp.1-12.
7. Xu, J., Sun, B. and Chen, B., 2019. A hybrid embedded discrete fracture model for simulating tight porous media with complex fracture systems. Journal of Petroleum Science and Engineering, 174, pp.131-143.
8. Zeng, Q., Yao, J. and Shao, J., 2020. An extended finite element solution for hydraulic fracturing with thermo-hydro-elastic–plastic coupling. Computer Methods in Applied Mechanics and Engineering, 364, p.112967.
9. Geng, S., Li, C., Zhai, S., Gong, Y. and Jing, M., 2023. Modeling the mechanism of water flux in fractured gas reservoirs with edge water aquifers using an embedded discrete fracture model. Journal of Energy Resources Technology, 145(3), p.033002.
10. Dong, Y., Zeng, B., Song, Y., Zhou, X., Li, P. and Zhang, F., 2023. Numerical Study of Hydraulic Fracture Propagation in Orthotropic Shale Reservoirs by Using the XFEM. Energy & Fuels.
11. Pezzulli, E., Nejati, M., Salimzadeh, S., Matthäi, S.K. and Driesner, T., 2022. Finite element simulations of hydraulic fracturing: A comparison of algorithms for extracting the propagation velocity of the fracture. Engineering Fracture Mechanics, 274, p.108783.
12. Paluszny, A., Salimzadeh, S. and Zimmerman, R.W., 2018. Finite-element modeling of the growth and interaction of hydraulic fractures in poroelastic rock formations. In Hydraulic Fracture Modeling (pp. 1-19). Gulf Professional Publishing.
13. Zhang, B., Guo, T., Qu, Z., Wang, J., Chen, M. and Liu, X., 2023. Numerical simulation of fracture propagation and production performance in a fractured geothermal reservoir using a 2D FEM-based THMD coupling model. Energy, 273, p.127175.
14. Zhang, Y., Hou, S., Mei, S., Zhao, Y. and Li, D., 2023. Finite volume method-based numerical simulation method for hydraulic fracture initiation in rock around a perforation. Journal of Zhejiang University-SCIENCE A, 24(1), pp.56-63.
15. Cheng, S., Zhang, M., Chen, Z. and Wu, B., 2022. Numerical study of simultaneous growth of multiple hydraulic fractures from a horizontal wellbore combining dual boundary element method and finite volume method. Engineering Analysis with Boundary Elements, 139, pp.278-292.
16. Yang, C.X., Yi, L.P., Yang, Z.Z. and Li, X.G., 2022. Numerical investigation of the fracture network morphology in multi-cluster hydraulic fracturing of horizontal wells: A DDM-FVM study. Journal of Petroleum Science and Engineering, 215, p.110723.
17. Wang, S., Yu, X., Winterfeld, P.H. and Wu, Y.S., 2023. Real-Time Simulation of Hydraulic Fracturing Using a Combined Integrated Finite Difference and Discontinuous Displacement Method: Numerical Algorithm and Field Applications. Water, 15(5), p.938.
18. Prieto, M., Aristizabal, J.A., Pradilla, D. and Gómez, J.M., 2022. Simultaneous numerical simulation of the hydraulic fractures geometry in multi-stage fracturing for horizontal shale gas wells. Journal of Natural Gas Science and Engineering, 102, p.104567.
19. Reddy, J.N. and Gartling, D.K., 2010. The finite element method in heat transfer and fluid dynamics. CRC press.
20. Mi, L., Jiang, H., Li, J., Li, T., Tian, Y., 2014. The investigation of fracture aperture effect on shale gas transport using discrete fracture model. Journal of Natural Gas Science and Engineering 21, 631-635.
21. Zhang, J., Mu, L., Jin, J. and Li, X., 2018. A computational method of productivity forecast of a multi-angle fractured horizontal well using the discrete fracture model. AIP Advances, 8(7): 075201.
22. Ozkan, E., Brown, M., Raghavan, R., Kazemi, H., 2011. Comparison of fractured-horizontal-well performance in tight sand and shale reservoirs. SPE Reservoir Evaluation & Engineering 14, 248-259.
23. Wang, H. (2018). Discrete fracture networks modeling of shale gas production and revisit rate transient analysis in heterogeneous fractured reservoirs. Journal of Petroleum Science and Engineering, 169, 796-812.
24. Zhao, Y.l., Liu, L.f., Zhang, L.-h., Zhang, X.Y., Li, B., 2019. Simulation of a multistage fractured horizontal well in a tight oil reservoir using an embedded discrete fracture model. Energy Science & Engineering 7, 1485-1503.
25. Cao M, Zheng S, Elliott B, Sharma MM. A novel integrated

DFN-fracturing-reservoir model: A case study. Rock Mechanics and Rock Engineering. 2023 Jan 27:1-5
26. Cao, M. and Sharma, M.M., 2023. A computationally efficient model for fracture propagation and fluid flow in naturally fractured reservoirs. Journal of Petroleum Science and Engineering, 220, p.111249.
27. Ranjbar, A., Izadpanahi, A. and Ebrahimi, A., 2022. Numerical analysis of geomechanical behavior of fractures and faults in a deformable porous medium. Journal of Petroleum Exploration and Production Technology, 12(11), pp.2955-2966.
28. RANJBAR, A., Izadpanahi, A., Ebrahimi, A. (2021). 'Numerical Analysis of Fluid Flow in a Deformable Porous Medium Using Finite Element Method', *Journal of Oil, Gas and Petrochemical Technology*, 8(Number 2), pp. 47-59. doi: 10.22034/jogpt.2022.277932.1094
29. Ranjbar, A., Hassani, H., Shahriar, K. and Shahrabi, M.J.A., 2020. Thermo-hydro-mechanical modeling of fault discontinuities using zero-thickness interface element. Journal of Rock Mechanics and Geotechnical Engineering, 12(1), pp.74-88.
30. Iranmanesh, M.A. and Pak, A., 2023. Three-dimensional numerical simulation of hydraulically driven cohesive fracture propagation in deformable reservoir rock using enriched EFG method. Computational Geosciences, 27(2), pp.317-335.
31. Ahmadi, Y. (2021). 'Relationship between Asphaltene Adsorption on the Surface of Nanoparticles and Asphaltene Precipitation Inhibition During Real Crude Oil Natural Depletion Tests', *Iranian Journal of Oil and Gas Science and Technology*, 10(3), pp. 69-82. doi: 10.22050/ijogst.2021.136325
32. Mansouri, M., Ahmadi, Y. and Jafarbeigi, E., 2022. Introducing a new method of using nanocomposites for preventing asphaltene aggregation during real static and dynamic natural depletion tests. Energy Sources, Part A: Recovery, Utilization, and Environmental Effects, 44(3), pp.7499-7513.
33. Mansouri, M., Parhiz, M., Bayati, B., Ahmadi, Y. (2021). 'Preparation of Nickel Oxide Supported Zeolite Catalyst (NiO/Na-ZSm-5) for Asphaltene Adsorption: A Kinetic and Thermodynamic Study', *Iranian Journal of Oil and Gas Science and Technology*, 10(2), pp. 63-89. doi: 10.22050/ijogst.2021.257740.1571
34. Ahmadi, Y. (2023). 'Improving Fluid Flow Through Low Permeability Reservoir in the presence of Nanoparticles: An Experimental Core Fooding WAG Tests', *Iranian Journal of Oil and Gas Science and Technology*, 12(2), pp. -. doi: 10.22050/ijogst.2021.287297.1595
35. Jafarbeigi, E., Ahmadi, Y., Mansouri, M. and Ayatollahi, S., 2022. Experimental core flooding investigation of new ZnO− γAl2O3 nanocomposites for enhanced oil recovery in carbonate reservoirs. ACS omega, 7(43), pp.39107-39121.
36. Ahmadi, Y., Mansouri, M. and Jafarbeigi, E., 2022. Improving simultaneous water alternative associate gas tests in the presence of newly synthesized γ-Al2O3/ZnO/Urea nano-composites: An experimental core flooding tests. ACS omega, 8(1), pp.1443-1452.
37. COMSOL, 2013. Multiphysics Model Library, Earth Science Module, Version 4.3a. COMSOL.
38. Yang, S., Wei, J., 2004. Reservoir physics. Beijing: Petroleum Industry Press, Chinese, 136-159.
39. Mahmoud, M., 2014. Development of a new correlation of gas compressibility factor (Z-factor) for high pressure gas reservoirs. Journal of Energy Resources Technology, 136(1), p.012903.
40. Wang, H., 2018. Discrete fracture networks modeling of shale gas production and revisit rate transient analysis in heterogeneous fractured reservoirs. Journal of Petroleum Science and Engineering, 169, pp.796-812.
41. Liu, S., Wei, J., Ma, Y., Liu, X. and Yan, B., 2021. Numerical simulation on the effect of fractures geometries for shale gas development with discrete fracture network model. Journal of Petroleum Exploration and Production, 11(3): 1289-1301.
42. Zeng, Q., Liu, W., Yao, J., Liu, J., 2020. A phase field based discrete fracture model (PFDFM) for fluid flow in fractured porous media. Journal of Petroleum Science and Engineering 191, 107191.

نشریه فناوری نفت، گاز و پتروشیمی، ۱۰(۲): ۱۵۲-۱۳۸، بهار و زمستان ۱۴۰۲

مقاله تحقیقاتی

پیش بینی تولید مخازن گاز شیل: تأثیر هندسه شکست هیدرولیک

علیرضا صادقی نیا [۱] محمد ترکمان [۲،*]

۱. دانشگاه شیراز، دانشکده شیمی، نفت و گاز، گروه مهندسی شیمی، شیراز، ایران

۲.دانشگاه شهید چمران اهواز، دانشکده مهندسی، گروه مهندسی شیمی، اهواز، ایران

مشخصات مقاله

تاریخچه مقاله:

دریافت: ۱۸ خرداد ۱۴۰۲

دریافت پس از اصلاح: ۴ آذر ۱۴۰۲

پذیرش نهایی: ۱۳ آذر ۱۴۰۲

کلمات کلیدی:

دینامیک سیالات محاسباتی

چاه افقی شکافدار

شبیه سازی عددی

شکاف هیدرولیک

مدل شکستگی گسسته

*عهده‌دار مکاتبات؛ محمد ترکمان

رایانامه:

M.torkaman@scu.ac.ir

تلفن: ۱۴-۳۳۲۲۶۶۰۰-۰۶۱

چکیده

مطالعه حاضر با استفاده از مدل گسسته شکاف به بررسی رفتار جریان گاز شیل در محیط های متخلخل شکافدار می پردازد. در این روش به منظور شبیه سازی حرکت جریان در محیط ماتریس و شکاف از یک مدل جدید که شامل قانون مکعب و معادله دارسی می باشد استفاده می شود. تاثیر دهانه شکست بر رفتار جریان با حل مجموعه ای از معادلات دیفرانسیل جزئی غیرخطی با استفاده از روش المان محدود شبیه سازی می شود. آنالیز حساسیت بر روی پارامترهای تاثیر گذار از جمله تعداد شکست هیدرولیک و نفوذ پذیری، دهانه شکست هیدرولیک و طول چاه بر روی بهره وری یک مخزن گاز شیل انجام می‌شود. نفوذپذیری شکست هیدرولیک با افزایش تولید نفت (بیش از دو برابر) بیشترین تأثیر را بر بازدهی چاه دارد. علاوه بر این، نتایج شبیه‌سازی نشان می‌دهد که افزایش تعداد شکستگی‌های هیدرولیک از ۴ به ۱۵ منجر به افزایش تولید بیش از دو برابر می‌شود. همچنین مشاهده می شود که نرخ تولید به دلیل وجود همبستگی مثبت بین اندازه دهانه شکستگی و ناحیه زهکشی افزایش می یابد. نتایج حاصل از این پژوهش اهمیت ویژگی‌های شکست هیدرولیکی و اثرات متعاقب آن بر بهره‌وری و امکان‌سنجی را نشان می‌دهد. به منظور اعتبارسنجی دقت مدل عددی، مقایسه بین توزیع فشار در یک مخزن شکسته منفرد و مدل شکست گسسته میدان فاز انجام می‌شود. نتایج عددی نشان می‌دهد که روش پیشنهادی از دقت قابل قبولی برخوردار می باشد..

نحوه استناد به این مقاله:

Sadeghinia A, Torkaman M., Predicting Production of Shale Gas Reservoirs: Impact of Hydraulic Fracture Geometry, Journal of Oil, Gas and Petrochemical Technology, 2023; 10(2): 137-152. DOI:10.22034/JOGPT.2024.401315.1121.